

Small Publications in Historical Geophysics

No. 6

**Analysis of Tidal Observations in the Arctic Ocean
made during the Vega Expedition**

Hans-Georg Scherneck & Martin Ekman

Summer Institute for Historical Geophysics
Åland Islands

1999

**Analysis of Tidal Observations in the Arctic Ocean
made during the Vega Expedition**

Hans-Georg Scherneck & Martin Ekman

Contents

1. Hibernation of the Vega in the pack-ice
2. Water depth measurements
3. Timing
4. Harmonic tide analysis
5. Looking at the residual
6. Comparisons with modern ocean tide models
7. Conclusions
- References

Summer Institute for Historical Geophysics
Åland Islands

1999

1. Hibernation of the Vega in the pack-ice

In 1878 - 1879 the famous Vega expedition in the Arctic Ocean took place. Vega was the name of the ship used, and the expedition was headed by the polar explorer A. E. Nordenskiöld, born in Finland but living and working in Sweden. The purpose of the expedition was to study the Arctic coast along Russian Siberia, parts of which were unknown and never mapped, and to find the possible North-East Passage around Europe and Asia, one of the great challenges of that time.

The Vega expedition turned out a great success. A general description was published by Nordenskiöld in two volumes in 1880 - 1881, and the scientific findings within different fields were published in five volumes during 1882 - 1887. A favourable event from the scientific point of view was the hibernation that the Vega was forced to by the pack-ice. This occurred at eastern Siberia in the Chukchi Sea, at a small place called Pitlekaj (between Wrangel Island and the Bering Strait); see Figures 1 and 2. The hibernation in the ice lasted for more than half a year. Most of that time was used for geophysical observations, especially meteorological, magnetic and oceanographic observations, which were performed mainly from November 1878 to June 1879. Moreover, astronomical observations allowed the accurate determination of the ship's position: latitude $67^{\circ} 04' 49''$ N, longitude $173^{\circ} 23' 02''$ W (Lindhagen, 1882). Strictly speaking this position should be reduced for the deflection of the vertical due to the geoid, but this is not important here.

The oceanographic observations are measurements of the ocean tide. The measurement technique, a table of the data obtained and some analysis carried out at the time have been published by Rosén (1887). The tide series acquired while the Vega was immobilised due to the sea ice is nearly flawless in coverage. Its value and usefulness as a mareographic record is the subject of this study. We will perform a tide analysis as well as make comparisons with modern tide models.

2. Water depth measurements

The tidal measurements commenced on 7 December 1878 and continued for precisely half a year, until 7 June 1879. Readings were made every hour. To illustrate the efficiency of the observation effort we show in Figure 3 the whole time series and, in order to discern individual samples, a blow-up of the month of April.

In order to measure the tides, a hole was cut in the ice at the stern of the Vega and kept open all through the winter. For a long time a seal resided

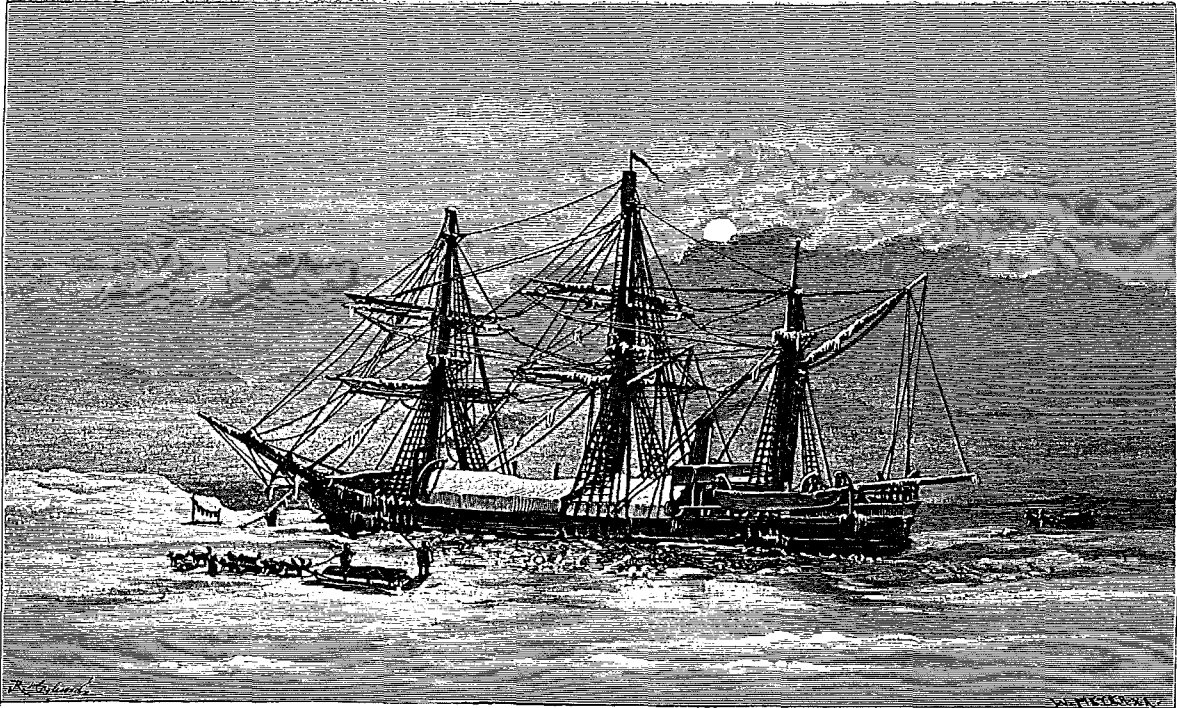


Figure 1. The Vega in the pack-ice (from Nordenskiöld, 1880).

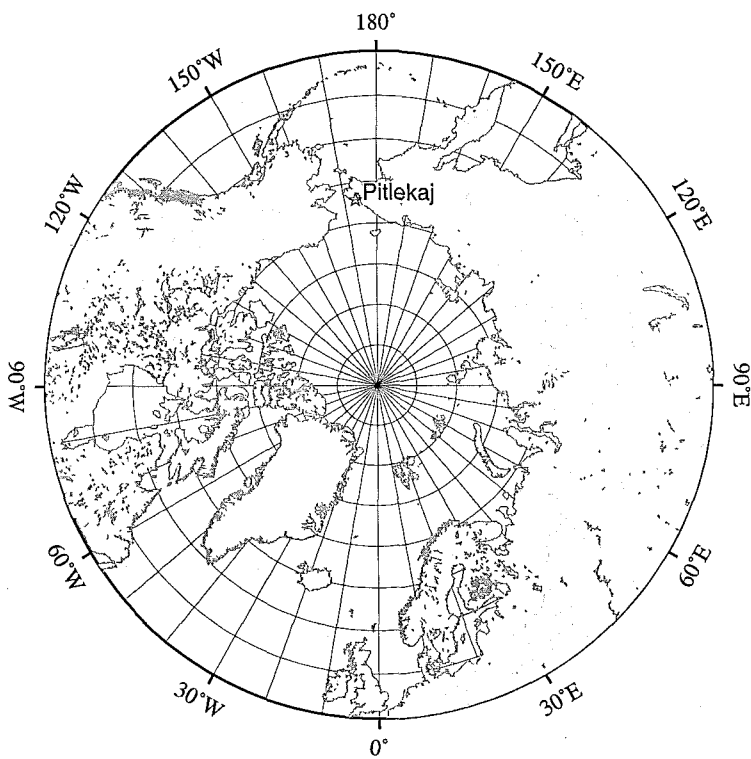


Figure 2. The location of Pitlekaj at the Arctic Ocean.

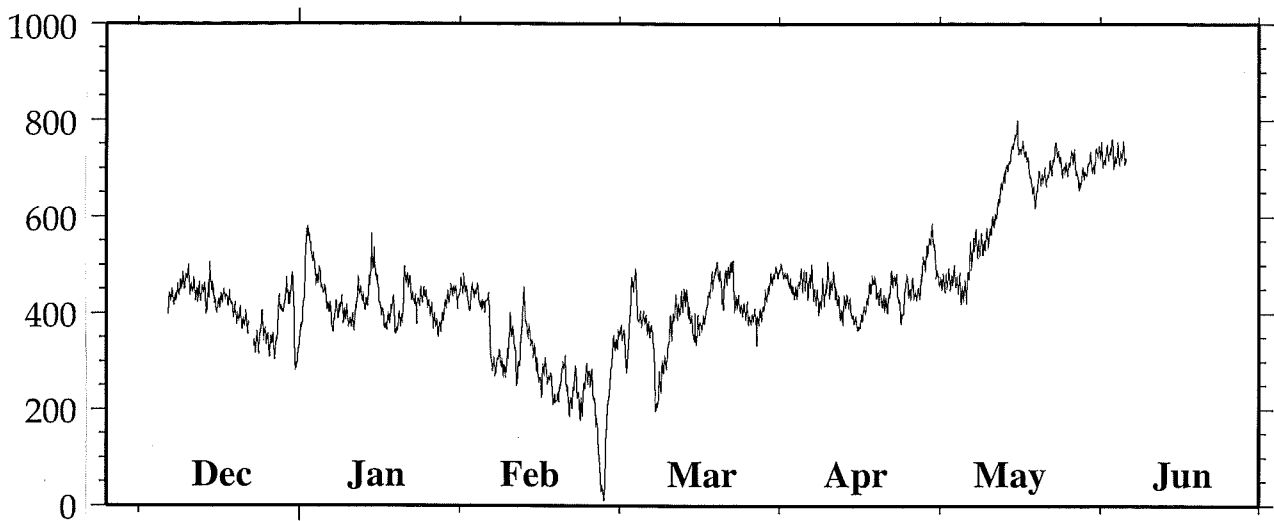


Figure 3a. The complete water level time-series of half a year, 1878 - 1879. (Units: months and decimal lines.)

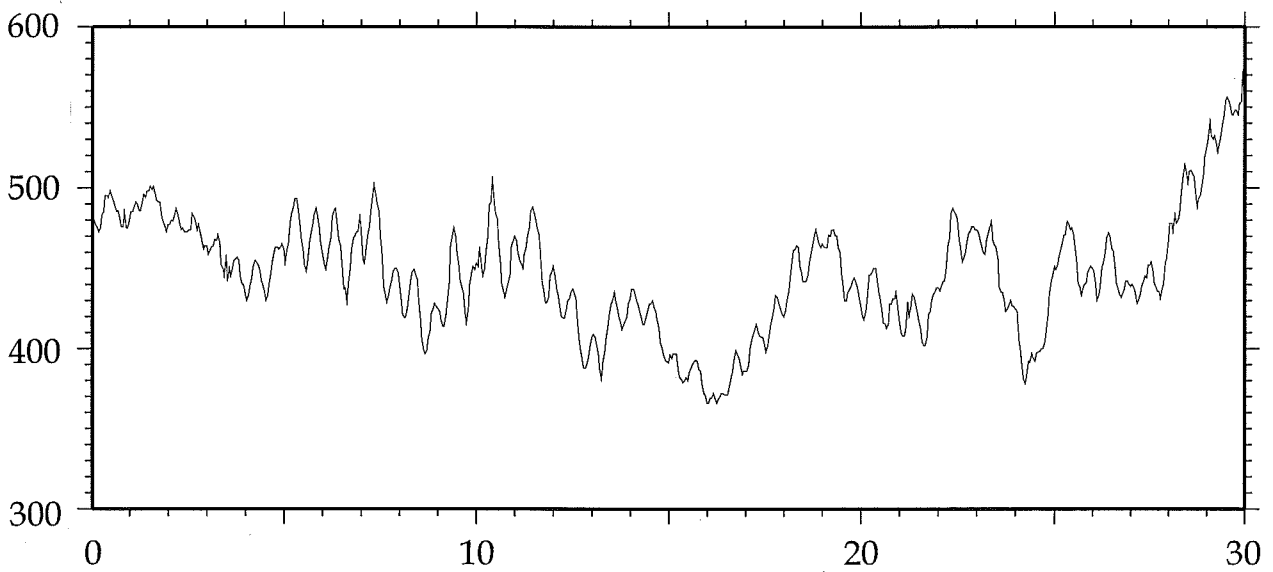


Figure 3b. The water level time-series for April 1879. (Units: days and decimal lines.)

there, making nice company for the crew. The observations, performed by the sea captain L. Palander, had to be made during severe weather conditions, normally at a temperature of minus 30 - 40 degrees Celsius in combination with strong northwesterly winds (Nordenskiöld, 1880).

The tide gauge measurements were made with a cable that was anchored at the sea bottom with cast-iron pigs. The cable ran into the Vega hull via a tube and over a wheel that had been firmly attached to a Vega boom. At the free end of the cable a cannon-ball served as a counterweight. A pointer was attached to the cable pointing at a scale graded in Swedish feet and decimals thereof.

The device is depicted in Rosén (1887). From the sketch a reader might conclude that the readings actually represent the negative of the water depth, or an arbitrary constant minus the depth. The question now arises whether the values published in Rosén's tables are the actual readings or readings converted with respect to the sign. This is an important point since a sign error will propagate and persist also in the estimated phases of the tides.

A clue may be found in Rosén's own way of analysing the data, where he makes a conversion of the sign in order to obtain sea level heights (he had, however, not participated in the expedition). Another clue could be contained in the tide analysis results themselves; if phases from one set of data are systematically closer to ocean model tides than for the opposite set of data we might favour the former. Anticipating the outcome: The published data lead to close agreement with the ocean model phases, whereas Rosén's sign-reversal would yield a 180° offset. Therefore, the tabulated values are almost certainly already reversed, and we have not converted them for sign.

Corrections to the readings before they entered into the tables (in addition to that for the sign) have been applied by the Vega crew to compensate for the varying water line of the floating vessel. A long-term effect due to a slow horizontal movement of the vessel towards a slightly deeper place has not been possible to correct for; this is reflected in Figure 3 where the increase in water depth during spring is caused by such a displacement of the ship.

The readings are tabulated in Swedish decimal lines. 1 decimal line = 1/10 of a decimal inch = 1/100 of a Swedish foot, the latter being 0.2969 m (Ohlon, 1974); this decimal system was introduced in Sweden as early as 1739. Hence we have transformed the tabulated readings to meters through the relation 1 decimal line = 0.02969 m.

3. Timing

It seems reasonable to assume that the Vega expedition timed their measurements from local solar time determinations. Local mean solar time was a viable concept in the 19th century; even railway stations along the same line used it, in Sweden until 1879. The crew may also have used their ship chronometre; in that case, Greenwich Mean Time (GMT) may have been applied. Hence there might be some doubt as to the notion of time in Rosén's (1887) tidal data record.

The most convincing clue here is the demarcation of the day and half-day boundaries that are termed midnight and midday, respectively, which suggests a local relation. Further, some time-series analysis was carried out by Rosén with a stacking method, using a basic solar day window length for the determination of solar amplitudes and phases, and equivalently one with the length of a lunar day in the case of lunar tides. When Rosén relates to a time lag of the tide he frequently uses the expressions for solar or lunar meridian transits. Thus, also in conjunction with these operations the text appears to speak rather of local relations than of such that would hold at the Greenwich zero meridian. Therefore, we have treated all times as local mean solar time.

Turning to more recent standards, local mean solar time (LMT) at Pitlekaj is related to UTC by $LMT = UTC + 12 \text{ h } 26 \text{ m } 28 \text{ s}$. In order to obtain a time equivalent to UTC for 1879, one can subtract 0.77 leap seconds per year, or 90 s in 120 years, to compensate for the retardation of the Earth's rotation. A semidiurnal tide advances in these 90 s by 0.77° , which is relatively small, but a one meter high tide changes by as much as 0.013 m during that time. A more accurate account of the deceleration of the earth rotation is not needed for a tidal analysis of data with a signal-to-noise ratio of less than 100:1.

As noted above, Pitlekaj is situated near the Bering Strait. Thus, there might be a question as to the date, since the longitude is west of Greenwich but, according to modern conventions, the Date Line has not been passed. However, from Nordenskiöld (1880) it is clear that dates "east of Greenwich" were used on board the Vega.

4. Harmonic tide analysis

The series expansion of the tide-generating forces employed for this study is the one by Tamura (1987). It contains roughly 1200 different tide waves and covers spherical harmonics to degree and order four. Response parameters are estimated that each relate a group of model waves to the local observations. The division into groups is based on the frequency resolution

capability, which is primarily dependent on the duration of the measurements. Our half a year of measurements, for instance, is sufficient to fully discriminate between the two declinational waves K_1 and P_1 (their beat period is 0.5 tropical years). The analysis is carried out for an elastic Earth with a liquid core; the latter introduces a resonant term in the tide-generating potential at diurnal periods (see e.g. Melchior, 1978).

The parameter estimation method uses a least-squares procedure. Since the premise of least-squares in this case is to determine sinusoidal wave packets in white noise (emphasis on white noise), the time series must be preconditioned in order to meet this criterion. In many cases of naturally occurring processes, long-term periodic or aperiodic variations are encountered. An efficient way to obtain white noise from a coloured noise process is by means of the maximum entropy method. From this one obtains a prediction error filter which is to be applied to both the time series and the model wave groups. Such filters designed for air pressure, water level or similar processes have typically five to ten coefficients, and their effect is to decorrelate subsequent data points. Deterministic filters like the Butterworth or Chebychev designs may yield a sharp suppression of unwanted signal components; however, their effect on the stochastic properties of time series is rather to distribute additional correlation between many samples even far apart from each other.

The particular least-squares solution method that is used here goes under the name of generalized inverse or Lanczos inverse (Aki & Richards, 1980); it has a near relationship to singular value decomposition. The advantage is that such methods are robust in situations of accidental overparametrization, like when model signals are virtually indistinguishable.

The results of the analysis are presented in Table 1, in the form of amplitude a and phase κ for each of the wave groups. The wave groups are represented by their most prominent members (central to the frequency band, large in magnitude), and the frequency ω is given along with the Darwin symbol (M_2 , O_1 etc.). The obtained harmonic constants for each wave i are related to the tidal height H at the time t through the well-known expression

$$H = \sum a_i \cos (\omega_i t - \kappa_i)$$

Although generally small, at the level of only a couple of centimeters, the most important semidiurnal tides - M_2 , S_2 , N_2 and K_2 - are well determined. The 95 percent confidence intervals amount to only a few millimeters. The largest semidiurnal tide wave is the lunar main tide M_2 with an amplitude as small as $a = 3.1 \pm 0.2$ cm. The diurnal tides appear still smaller. In that

Table 1. Harmonic constants resulting from the tide analysis: amplitudes (a , in cm) with 95 % confidence intervals, and phases (κ , in degrees) counted as lag angles relative to the tide potential at the zero meridian. Also shown are frequencies (ω , in cycles per day). The statistically significant results are denoted by stars.

Wave	ω	$a \pm 95 \%$	κ
M _m	0.0363	3.56 \pm 4.16	56.5
M _f	0.0732	1.41 \pm 3.00	128.1
Q ₁	0.8932	0.52 \pm 0.62	233.7
O ₁	0.9295	1.34 \pm 0.61 *	245.0
M ₁	0.9664	0.12 \pm 0.48	310.5
P ₁	0.9973	0.49 \pm 0.60	242.2
K ₁	1.0027	1.53 \pm 0.56 *	229.8
J ₁	1.0390	0.29 \pm 0.51	245.7
OO ₁	1.0759	0.06 \pm 0.35	203.1
2N ₂	1.8645	0.12 \pm 0.18	139.4
N ₂	1.8960	0.85 \pm 0.23 *	128.3
M ₂	1.9323	3.07 \pm 0.23 *	172.4
L ₂	1.9686	0.06 \pm 0.22	317.0
S ₂	2.0000	1.02 \pm 0.21 *	236.1
K ₂	2.0055	0.24 \pm 0.18 *	296.3
M ₃	2.8984	0.09 \pm 0.14	9.9
S ₃	3.0000	0.09 \pm 0.14	62.2
K ₃	3.0082	0.04 \pm 0.14	47.6

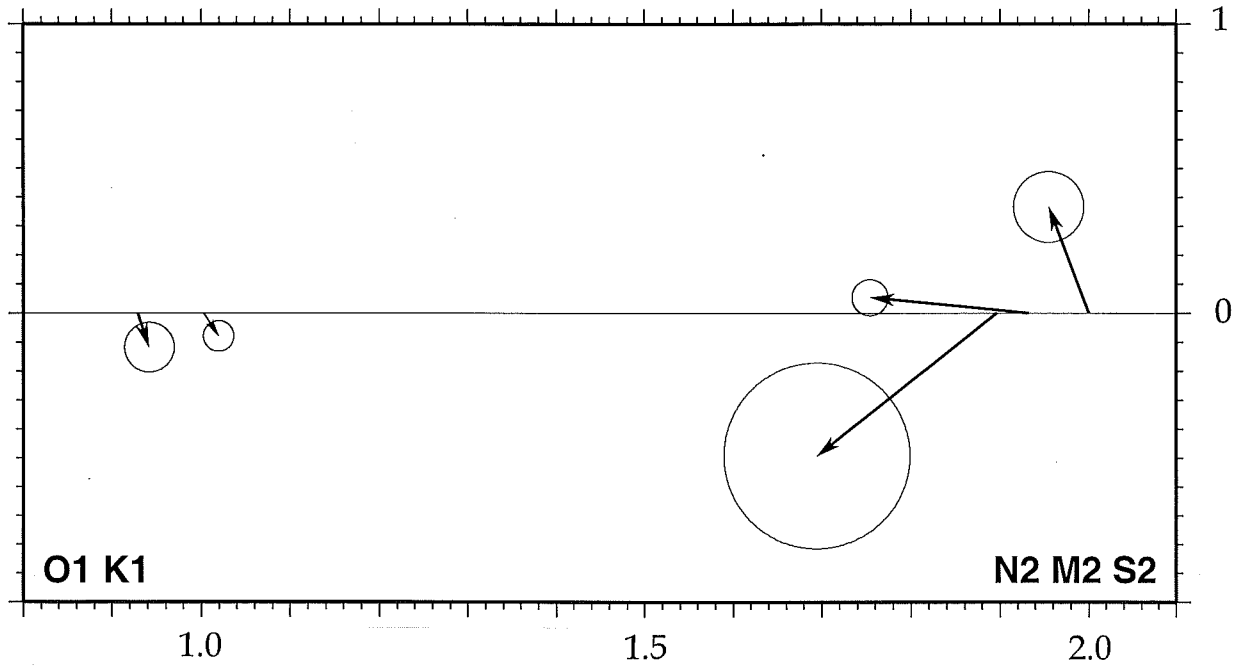


Figure 4. Gain spectrum for the statistically significant tides of Table 1, except the small K_2 tide. Each tide (arrow foot) is identified by its frequency (along the abscissa). The length of each arrow corresponds to the gain factor (measured according to the ordinate scale), and its angle from the abscissa corresponds to the phase lag relative to the local tide potential.

frequency band, only two waves show up above the noise level: O_1 and K_1 , their amplitudes not exceeding 1.5 cm.

Already Rosén (1887), limiting his study to the semidiurnal lunar and solar main tides M_2 and S_2 , noticed that these tides are small. His interpretation of this was that the unknown sea north of the Bering Strait could not be very large. At that time, however, the general amphidromic (nodal) character of the tides due to resonance was not yet known; this became clear through Harris' (1904) investigations (see also Ekman, 1993). The realistic interpretation of the small amplitudes found above is that the Vega was located close to a tidal node.

Of the long-period tides, the annual one (S_a) and the semiannual one (S_{sa}) are highly uncertain as the signal duration is precisely 0.5 years, and long-periodic noise is strongly present. Thus, these results were suppressed. The monthly tide M_m and the fortnightly tide M_f are found at insignificant amplitudes.

The harmonic results can also be shown in the form of gain factors, by dividing the ocean tide amplitudes by the amplitudes of the tide potential (the equilibrium amplitudes). The result usually shows a slight frequency dependence across a tide band. The tide response of an ocean area can be described as a superposition of resonant modes, much like the resonant strings that a number of musical instruments possess (sitar, certain guitars and lutes, the Swedish key harp etc.). The excitation process in each case is a compound signal with a finite number of slightly distorted sinusoids, and the resonant strings or oceanic oscillatory systems contribute to the compound response in reciprocal proportion to the difference in frequency. The richer the resonant structure of the ocean area is, or the number of resonant strings, the richer of features is the gain spectrum. However, a detailed study of the gain spectrum requires a high signal-to-noise ratio of the measurements. The present data set is a bit limited in this respect. We show the gain spectrum in Figure 4 for those tides that are statistically significant at the 95 percent level. The result clearly illustrates that all amplitudes are reduced, particularly the diurnal ones.

5. Looking at the residual

After the least-squares tidal fit the postfit residual appears to be mostly white noise, i.e. fulfill the normal error criterion; see Figure 5. The variance parameter for the least-squares has been taken from the RMS of the series shown here, as a kind of hindsight justification in lieu of a priori information about the measurement error. If one considers the variable sea level as part of the noise of the measurement process, then only the hindsight variance is

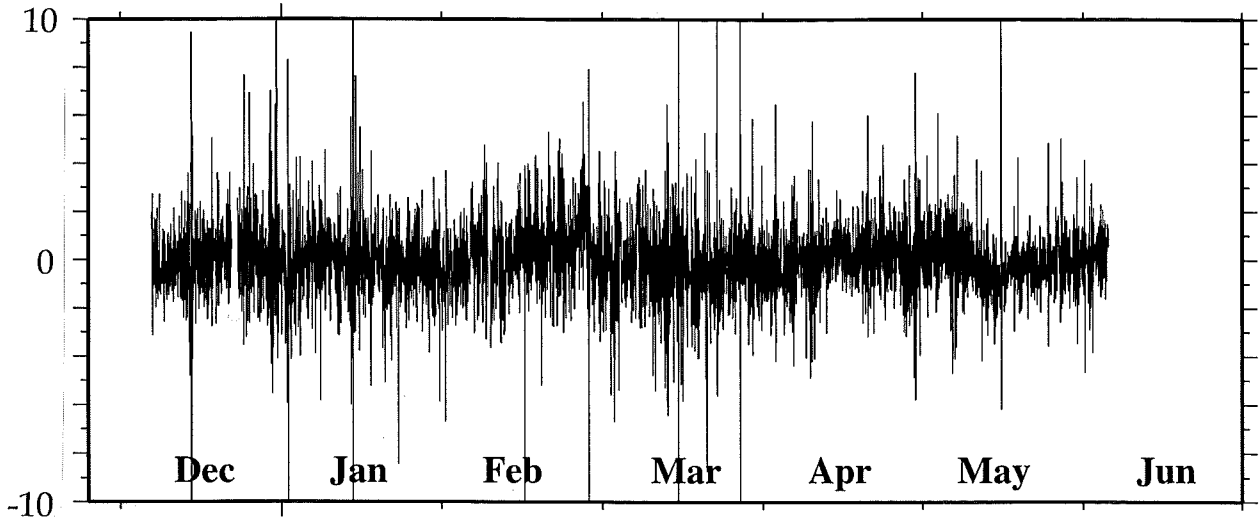


Figure 5. Filtered residual of the complete water level time-series. (Units: months and cm.)

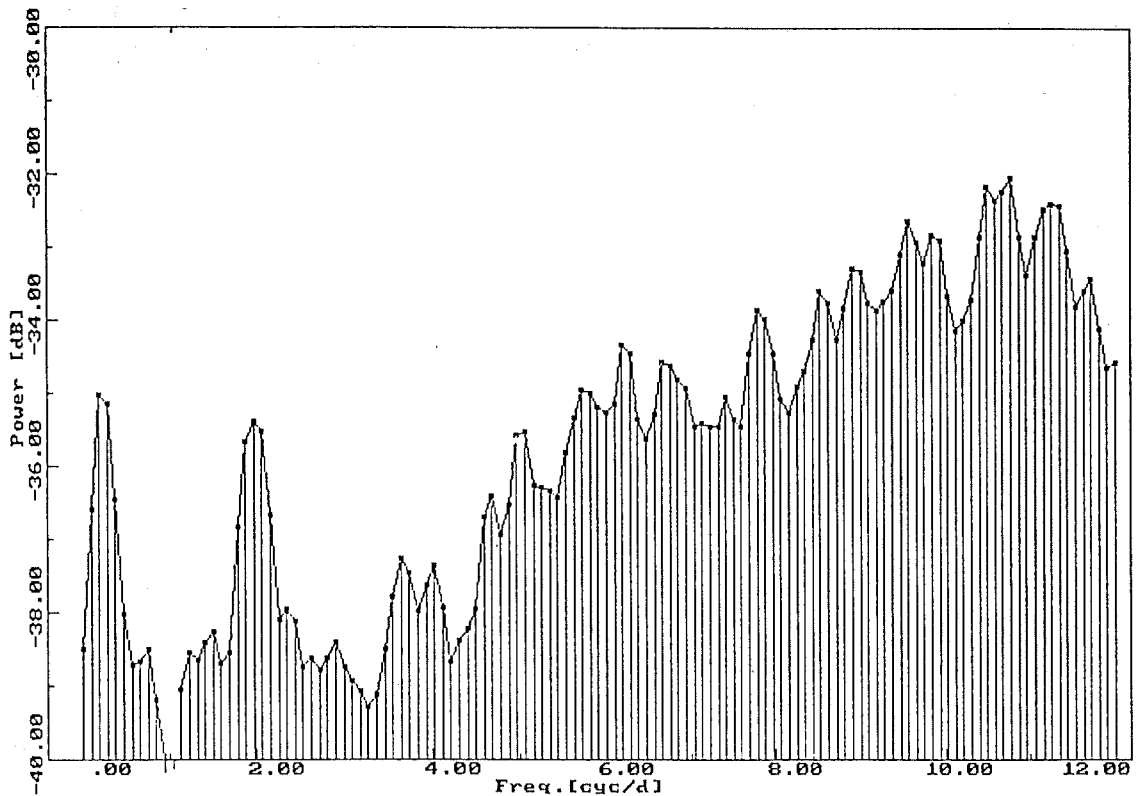


Figure 6. Power spectrum of the filtered residual. (Units: cycles/day and dB.)

objectively available; the reading error of the scale would probably be an overoptimistic guess.

In order to judge the efficiency of the least-squares fit, the residual is analysed with standard time-series analysis techniques (e.g. Oppenheim and Schafer, 1975). Power spectrum analysis shows that the residual is a little overwhitened, and that there is residual semidiurnal spectral power; see Figure 6. The reason for this is most often that there are temporary perturbations, like solar synchronous thermal tides that affect the measurements only during days with clear skies, time-varying calibration of the measurement device, or nonlinearity effects. There might also be other reasons, like not exactly repetitive patterns in daily human activities on board the ship. The overwhitening, i.e. the exaggerating action of the prediction error filter, is a direct consequence of these nonstationary signal components.

6. Comparisons with modern ocean tide models

The local coastline of the Arctic Ocean near Pitlekaj is fairly complicated. In order to resolve the basin geometry, a 1 x 1 degree grid as in the case of the Schwiderski (1980) tide model is not fine enough. Also the 0.5 x 0.5 degree grid of Le Provost et al. (1994) does not have the sufficient resolving power to obtain continuity between the tide in the bay close to Pitlekaj and the open Arctic Ocean. The Schwiderski model is based on tide gauge results and hydrodynamic interpolation, while Le Provost et al. used a completely observation-free hydrodynamic finite element model. The latter has a variable mesh density; by this it could resolve small-scale features on the shelves. However, for more convenient use the finite element mesh is resampled on a regular 0.5 x 0.5 degree grid and some detail is lost. Table 2 shows the most important diurnal and semidiurnal tides, comparing the two models with the results of our analysis.

The Schwiderski (1980) model is very close to the observed tides, both in amplitude and phase. According to Schwiderski's original maps the coastal nodes within $\pm 5^\circ$ longitude from Pitlekaj are hydrodynamically interpolated (unconstrained), as no tide gauge data from this area appear to have been available to him. This model does not represent the bay.

The model of Le Provost et al (1994) predicts systematically exaggerated amplitudes but not unreasonable phases. The exaggeration in amplitude, especially for the semidiurnal tides, is particularly evident for the bay, which is closest to the actual location. For the open ocean just to the north of the bay, which might be more representative for the actual location, the model yields smaller amplitudes. Nevertheless, they are still too large by a factor two.

Table 2. Comparisons of the tide models of Schwiderski (1980), denoted S, and Le Provost et al (1994), denoted L, with the statistically significant results from Table 1, denoted T. The lower L solution represents the bay. Amplitudes (a) are given in cm, phases (κ) in degrees.

Wave	$a(T)$	$a(S)$	$a(L)$	$\kappa(T)$	$\kappa(S)$	$\kappa(L)$
M ₂	3.1	3.5	4.0	172.4	162.6	145.2
S ₂	1.0	1.1	1.9	236.1	226.5	193.0
N ₂	0.8	0.7	1.1	128.3	124.1	134.9
K ₂	0.2	0.2	0.5	296.3	187.7	197.9
O ₁	1.3	1.0	1.6	245.0	245.0	241.6
(P ₁	0.5	0.6	0.7	242.2	261.4	233.2)
K ₁	1.5	1.6	3.2	229.8	255.5	240.1
M ₂			12.7			224.9
S ₂			6.7			276.7
N ₂			3.8			201.1
K ₂			2.0			286.7
O ₁			2.4			261.6
(P ₁			1.1			253.0)
K ₁			5.2			261.3

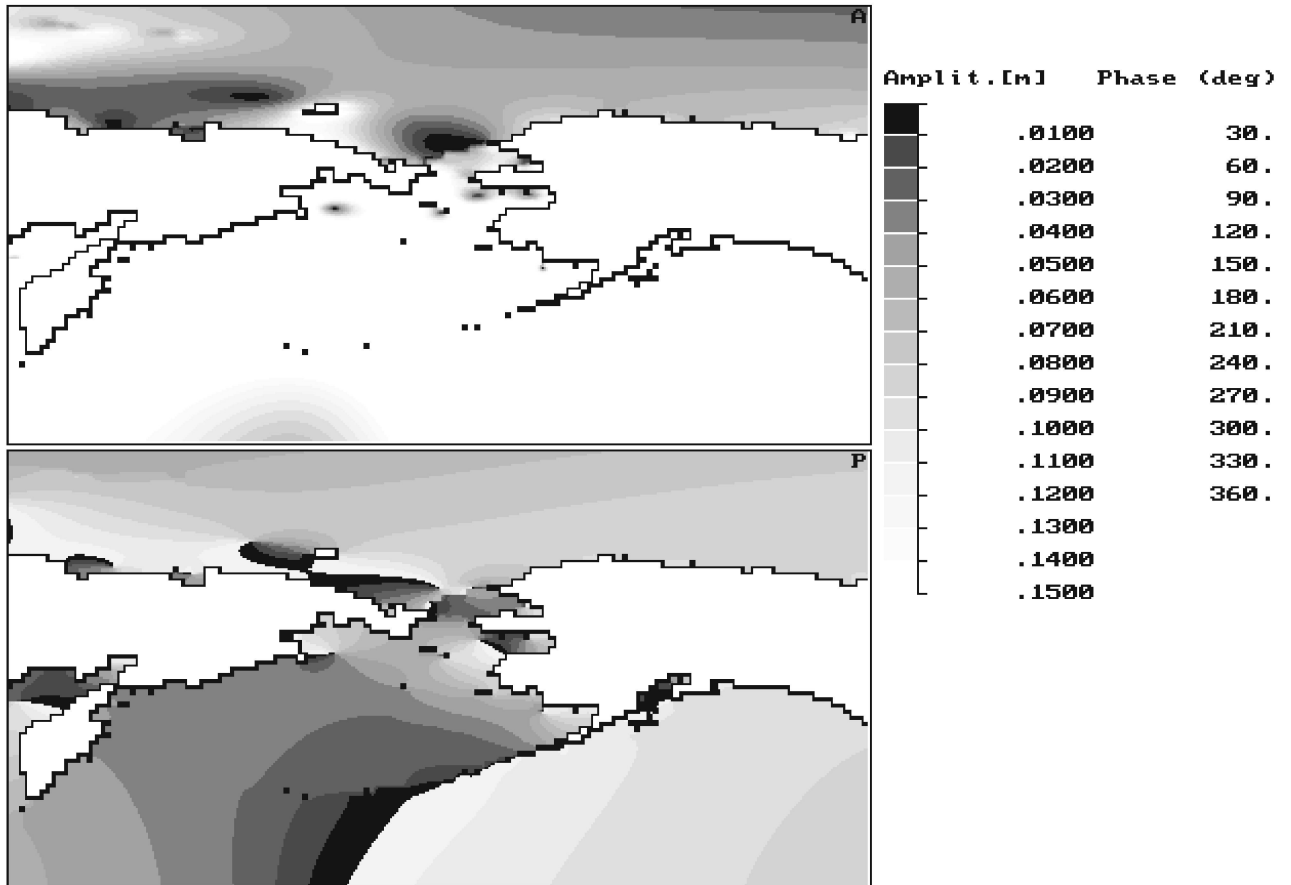


Figure 7. The M_2 tide (amplitudes and phases) around Siberia, the Bering Strait and Alaska according to the model of Le Provost et al (1994). (For the location of Pitlekaj see Figure 2.)

The large difference in the model of Le Provost et al between the tide in the bay and in the ocean appears to point out a problem, either in the original finite element solution or in the resampling. Bays that are connected to open waters through a strait often follow passively the open ocean tide just outside the mouth, except in rare cases of large bays with very narrow and shallow mouths (choking) or long bays with small depths (resonance). In the model, the bay might have been connected through only a single point, which may introduce large local errors in the solution. The model amplitude of the main semidiurnal tide M_2 at Pitlekaj and its neighbourhood is about twice or three times as large as the small amplitude from our analysis. The observed node here might be connected to a larger node (amphidromic area) north of the Bering Strait seen in the M_2 overview in Figure 7.

We thus find that modern tide models do have problems in the area in question, and that the Vega analysis might actually contribute valuable information for constructing an improved regional tide model. Constructing such a model, however, would digress too far from the subject of the present study.

7. Conclusions

The Arctic tide observations performed during the Vega expedition in 1878 - 1879 are of a surprisingly high quality, especially considering the severe conditions under which they were made. The analysis yields a 95 percent confidence level of 0.2 cm for semidiurnal tides and somewhat more for diurnal ones. All tide amplitudes are small, indicating closeness to a node. The semidiurnal tides are a couple of centimeters, the lunar main tide M_2 reaching 3.1 cm, while the diurnal ones are even somewhat smaller.

We have found that modern ocean tide models have problems in the area, and that the above Vega tide analysis might actually contribute valuable information for constructing an improved regional tide model.

References

- Aki, K, & Richards, P G (1980): Quantitative seismology; theory and methods, 2. W H Freeman & Co, 559-935.
- Ekman, M (1993): A concise history of the theories of tides, precession-nutation and polar motion (from antiquity to 1950). *Surveys in Geophysics*, 14, 585-617.
- Harris, R A (1904): Manual of tides, 4B. Report of the United States Coast and Geodetic Survey.
- Le Provost, C, Genco, M L, Lyard, F, Vincent, P, Canceil, P (1994): Spectroscopy of the world ocean tides from a finite element hydrological model. *Journal of Geophysical Research*, 99 C, 24777-24798.
- Lindhagen, A (1882): Vega-expeditionens geografiska Ortsbestämningar. Vega-expeditionens vetenskapliga iakttagelser, 1, 453-471.
- Melchior, P (1978): The tides of the planet Earth. Pergamon Press, 609 pp.
- Nordenskiöld, A E (1880): Vegas färd kring Asien och Europa, 1. Stockholm, 510 pp. Also English translation (1880): The Voyage of the Vega. London. (This book was published in 11 languages.)
- Ohlson, R (1974): Gamla mått och nya. Sohlmans förlag, 191 pp.
- Oppenheim, A V, & Schaffer, R W (1975): Digital signal processing. Prentice Hall, 585 pp.
- Rosén, P G (1887): Iakttagelser af tidvattnet vid Pitlekaj under Vega-expeditionen 1878-79. Vega-expeditionens vetenskapliga iakttagelser, 5, 513-535.
- Schwiderski, E W (1980): On charting global ocean tides. *Reviews of Geophysics and Space Physics*, 18, 243-268.
- Tamura, Y (1987): A harmonic development of the tide-generating potential. *Marées Terrestres - Bulletin d'Informations*, 99, 6813-6855.
- Wessel, P, & Smith, W H F (1995): New version of the Generic Mapping Tools released. *EOS - Transactions of the American Geophysical Union*, 76, p 329.

Acknowledgements

Britt-Marie Ekman has kindly transferred the Vega tidal records in the Rosén paper to computer readable form. Graphic procedures have been provided by Wessel and Smith (1995).

Ordinary addresses of the authors

Hans-Georg Scherneck, Onsala Space Observatory, SE - 439 92 Onsala, Sweden.

Martin Ekman, Geodetic Research Division, National Land Survey, SE - 801 82 Gävle, Sweden.